Journal of Biomolecular NMR, 6 (1995) 141–152
ESCOM

J-Bio NMR 289

Backbone assignment, secondary structure and Protein A binding of an isolated, human antibody VH domain

Lutz Riechmann* and Julian Davies

MRC Laboratory of Molecular Biology, Hills Road, Cambridge CB2 2QH, U.K.

Received 20 January 1995
Accepted 12 May 1995

Keywords: Human immunoglobulin; Camel; Detergent; Protein A; Heteronuclear NMR; Secondary structure

Summary

Antibody heavy chain variable domains (VH) lacking their light chain domain (VL) partner are prime candidates for the design of minimum-size immunoreagents. To obtain structural information about isolated VH domains, a human VH was labelled with ^{15}N or doubly labelled with both ^{15}N and ^{13}C and was studied by heteronuclear nuclear magnetic resonance spectroscopy. Most (90%) of the ^{1}H and ^{15}N main-chain signals were assigned through two-dimensional TOCSY and NOESY experiments on the unlabelled VH and three-dimensional heteronuclear multiple quantum correlation TOCSY and NOESY experiments on the ^{15}N-labelled VH. Four short stretches of the polypeptide chain could only be assigned on the basis of three-dimensional HNCA and HN(CO)CA experiments on the ^{13}C-/^{15}N-labelled protein. Long-range interstrand backbone NOEs suggest the presence of two adjacent β-sheets formed by altogether nine antiparallel β-strands. $^{3}J_{NHC^{\alpha}H}$ coupling constants and the location of slowly exchanging backbone amides support this interpretation. The secondary structure of the isolated VH is identical to that of heavy chain variable domains in intact antibodies, where VH domains are packed against a VL domain. The backbone assignments of the VH made it possible to locate its Protein A binding site. Chemical shift movements after complexing with the IgG binding fragment of Protein A indicate binding through one of the two β-sheets of the VH. This β-sheet is solvent exposed in intact antibodies. The Protein A binding site obviously differs from that on the Fc portion of immunoglobulins and is unique to members of the human VH_{III} gene subgroup.

Introduction

Monoclonal antibodies (Köhler and Milstein, 1975) are widely used in basic research and clinical medicine to specifically target antigens and objects presenting them. Recombinant DNA technology enables the in vitro design of purpose-built immunoglobulins (reviewed in Winter and Milstein, 1991; Sandhu, 1992). One of the aims in that respect is the generation of antigen-specific immunoreagents of minimum size. Smaller antibody fragments exhibit a faster biodistribution and improved clearance rate in clinical applications (Colcher et al., 1990; Yokota et al., 1992; Nedelman et al., 1993). Antigen binding sites of antibodies are formed by a pair of light and heavy chain variable domains (VL and VH). Expression of VH and VL without their constant domains yields the Fv fragment, which has the same antigen specificity as the original antibody (Riechmann et al., 1988; Skerra and Plückthun, 1988). Although Fv fragments are usually viewed as the smallest unit able to form complete antigen binding sites, early observations (Harber and Richards, 1966; Rockey, 1967; Jaton et al., 1968) indicated that in

*To whom correspondence should be addressed.

Abbreviations: CDR, complementarity determining region; CHAPS, [(cholamidopropyl)-dimethylammonio]-1-propanesulfonate; DQF-COSY, double-quantum-filtered correlated spectroscopy; Fab, antigen binding antibody fragment; Fc, crystallisable antibody fragment; Fv, heterodimer of VH and VL; H1 (2, 3), hypervariable loop 1 (2, 3); IgG, immunoglobulin G; NOE, nuclear Overhauser effect; NOESY; nuclear Overhauser enhancement spectroscopy; HMQC, heteronuclear multiple quantum correlation spectroscopy; HSQC, heteronuclear single quantum correlation spectroscopy; scFv, single chain Fv; TOCSY, total correlation spectroscopy; TPPI, time-proportional phase incrementation; VH, antibody heavy chain variable region; VL, antibody light chain variable region. Mutants are denoted by the wild-type amino acid (one-letter code), followed by the residue number and the new amino acid.

some cases VH domains retain a significant part of the original binding activity. VH domains with high antigen affinity were also detected in expression libraries derived from immunised mice (Ward et al., 1989). More recently, natural, antigen-binding antibodies lacking light chains were found in camels (Hamers-Casterman et al., 1993; Muyldermans et al., 1994). Isolated human antibody VH domains, specific for hapten and protein antigens, have also been engineered in vitro after expression and selection on the surface of phage (Davies and Riechmann, 1995).

Structures of VH domains associated with their VL partner have been solved by X-ray crystallography of Fab fragments (Alzari et al., 1988; Colman, 1988), which consist of VH and VL attached to a constant domain. NMR studies on VH domains as part of Fv fragments were undertaken by labelling with ^{15}N and ^{13}C to various degrees (Wright et al., 1990; Riechmann et al., 1991; Takahashi et al., 1992; Freund et al., 1994), but have not yet resulted in complete assignments or structures because of problems with solubility and line widths. Even widespread assignments through amino acid-specific labelling (Freund et al., 1994) might not result in detailed structural information, due to sensitivity problems in NOE experiments.

Studies on isolated VH domains proved difficult, as they usually express poorly on their own and aggregate (Riechmann, L., unpublished results; Davies and Riechmann, 1994). Based on the sequences of the camelid VH domains, which occur naturally without VL partners, we modified a human VH domain to improve its solubility. Three mutations in the VH/VL interface, together with the addition of the detergent CHAPS, resulted in an improvement of the average NMR proton line width from 22 to 11 Hz (Davies and Riechmann, 1994). Here we show that the improvement in line width facilitates assignment of all main-chain ^{1}H, ^{15}N and $^{13}C^{\alpha}$ resonances and determination of the secondary structure of the VH domain.

The assignments made it possible to locate the Protein A binding site on the VH, based on amide chemical shift changes after complex formation with the IgG binding fragment of Protein A. This Protein A binding site is unique to antibodies or antibody fragments containing heavy chain variable domains originating from the human VH_{III} subgroup of genes (Sasso et al., 1991).

Materials and Methods

Protein expression and purification

The VH-P8 protein is based on a human VH domain derived from the scFv αOx13 (Hoogenboom and Winter, 1992). The isolated VH does not bind the ligand (2-phenyloxazol-5-one) of the scFv. Mutations (VH-G44E, L45R, W47I) introduced in VH-P8 to improve its NMR line width have been described previously (Davies and Riechmann, 1994). Unlabelled VH was prepared using a pUC19-based expression vector (McManus and Riechmann, 1991). To prepare uniformly ^{15}N-enriched and uniformly doubly ^{15}N- and ^{13}C-labelled protein, the VH gene linked to the leader sequence of the pectate lyase B gene was subcloned into a modified pET11 vector (Riechmann et al., 1991). The vector was expressed in the *Escherichia coli* strain BL21-DE3, using rich medium (CELTONE, Martek) diluted three- (^{15}N-labelling) or twofold (^{15}N-/^{13}C-labelling) with nitrogen-depleted M9 salts and supplemented with 100 mg/l ampicillin and, for the ^{15}N-enriched sample, 1% glycerol. Bacterial cultures were grown in 6 ml aliquots at 37 °C as a 1/100 dilution of an overnight culture inoculated from a fresh ampicillin plate. After 8 h, cultures were induced with 1 mM isopropyl-β-D-thiogalactopyranoside at 25 °C for another 20 h. VH was purified from the culture supernatants using Protein A Sepharose (Davies and Riechmann, 1994). From 1 l of the (undiluted) commercial ^{15}N and $^{15}N/^{13}C$ medium, 27 mg and 8 mg of VH were purified, respectively.

NMR samples were prepared by concentration and extensive washing on a YM3 membrane (Amicon). The final buffer contained 10 mM pyrophosphate, 200 mM NaCl, pH_{app} 6.2, in either 99.9% D_2O or 92% H_2O/8% D_2O. The final protein concentration of both the ^{15}N-labelled and the unlabelled samples was ~1.7 mM. The concentration of the doubly ^{15}N-/^{13}C-labelled protein was ~1.3 mM. 3-[(Cholamidopropyl)-dimethylammonio]-1-propanesulfonate (CHAPS) was added to achieve a sixfold molar excess of detergent over VH. The complex of the VH with complete, secreted Protein A from *Staphylococcus aureus* (Sigma, P0631) or a recombinant IgG-binding fragment of Protein A (Sigma, P4422) was formed by mixing a 0.3 mM ^{15}N-labelled VH sample with 10 mg or 5 mg Protein A fragment in a volume of 480 µl. Mixtures were transferred into the buffer described above by washing on a YM3 membrane; a sixfold molar excess of detergent was added.

NMR spectroscopy

Unless otherwise stated, NMR experiments were performed at 303 K on a Bruker AMX-500 spectrometer using either a double or a triple resonance 5 mm probe. Homonuclear 2D NOESY (Jeener et al., 1979; $\tau_m = 100$ ms), TOCSY (Braunschweiler and Ernst, 1983; $\tau_m = 48$ ms) and DQF-COSY (Rance et al., 1983) experiments on the unlabelled sample were acquired with 2048 complex t_2 points (spectral width 12 500 Hz), 460 real t_1 points (spectral width 5300 Hz) and 64 scans per increment, using time-proportional phase incrementation (TPPI) (Marion and Wüthrich, 1983). During the relaxation delay of 0.9 s, the water signal was presaturated.

With the ^{15}N-enriched sample, 2D ^{15}N-^{1}H HSQC

(Bodenhausen and Ruben, 1980) and 3D ^{15}N-^{1}H NOESY-HMQC (τ_m = 100 ms) and TOCSY-HMQC (τ_m = 63 or 33 ms) experiments were acquired using solvent suppression via spin-lock pulses (Messerle et al., 1989), plus additional weak presaturation of the H_2O signal during the 0.9 s relaxation delay. For the TOCSY experiment, a modified DIPSI-2 sequence for a clean TOCSY (Cavanagh and Rance, 1992) was used. The 3D NOESY and TOCSY experiments were acquired with 1024 complex t_3 points (spectral width 8064 Hz) and 256 real points in the indirect ^{1}H dimension (t_1, spectral width 4000 Hz) using 32 scans per increment. For the doubly ^{15}N-/^{13}C-labelled VH, a refocussed 3D HNCA (Farmer et al., 1992) and a 3D HN(CO)CA spectrum (Grzesiek and Bax, 1992) were acquired with 50 real points in the ^{13}C dimension (spectral width 4275 Hz) and 64 (HNCA) or 32 (HN(CO)CA) scans per increment. For 3D experiments, 60 complex points were recorded in the ^{15}N dimension for a spectral width of 1525 Hz. Quadrature detection in the 3D experiments was achieved using TPPI for the indirect ^{1}H or ^{13}C dimension and TPPI/States (States et al., 1982) for the ^{15}N dimension. $^{3}J_{NHC^{\alpha}H}$ coupling constants were estimated from J splittings of cross peaks in F1 columns, extracted from an HMQC spectrum recorded with 600 increments (1525 Hz spectral width) in the ^{15}N dimension, as described previously (Kay and Bax, 1990). For ^{15}N decoupling, the GARP (Shaka et al., 1985) composite pulse sequence was applied during acquisition of all heteronuclear experiments. ^{1}H chemical shifts were referenced to an external TSP standard; ^{15}N and ^{13}C chemical shifts were referenced indirectly (Live et al., 1984). The ^{1}H carrier frequency was set to that of water (4.75 ppm), the ^{15}N carrier frequency was set to 118 ppm and the ^{13}C carrier frequency to 53.5 ppm (C^{α} pulses) or 172 ppm (carbonyl pulses).

Spectra were processed with UXNMR (Bruker) or FELIX (Biosym) software. Using FELIX software routines, low-frequency deconvolution was employed to remove the water signal and 3D data were zero-filled twice in F3 and F1, and extended by 25% in F2 using linear prediction. Data were typically multiplied with a 65° shifted sine-bell function before Fourier transformation. Prior to peak picking, an automated baseline flattening was performed.

Results and Discussion

Assignment

Resonance assignment of the modified human VH domain VH-P8 by homonuclear NMR techniques alone is unlikely to succeed. The domain consists of 117 amino acid residues and its NMR analysis requires the presence of a three- to sixfold molar excess of the detergent CHAPS over the VH to reduce its line width (Anglister et al., 1993; Davies and Riechmann, 1994). More than a 10-fold excess of CHAPS over VH is disadvantageous, as parts of the VH adopt a second conformation without further improvement in line width. Under these conditions, two NH signals were observed for several residues in β-strand C' of β-sheet 2 (L. Riechmann, unpublished results). A sixfold molar excess of detergent causes small chemical shift changes for many VH proton signals, but homonuclear 1D spectra look overall very similar. The structure of the VH seems therefore principally undisturbed. More details about the effect of CHAPS on the VH are difficult to obtain, because the line width of the VH signals in the absence of the detergent already compromises ^{1}H-^{15}N HSQC experiments. VH protein also starts to irreversibly aggregate at concentrations required for NMR experiments if no CHAPS is present.

Therefore, heteronuclear NMR techniques on the ^{15}N- and the ^{13}C-/^{15}N-enriched VH were used for the backbone assignment and the determination of its secondary structure. Complete side-chain assignments cannot be obtained from homonuclear experiments, as the strong signals from the aliphatic CHAPS protons obscure many VH side-chain resonances. However, complete side-chain resonance assignments based on HCCH-COSY (Bax et al., 1990a), HCCH-TOCSY (Bax et al., 1990b), C(CO)NH and H(CCO)NH (Grzesiek et al., 1993) experiments performed on the doubly labelled VH will eventually enable a tertiary structure determination using ^{15}N- and ^{13}C-resolved ^{1}H NOE data (Clore and Gronenborn, 1991).

Initially, only a ^{15}N-enriched VH was available and assignment was possible for most residues based solely on ^{15}N-resolved data. For 105 out of the 117 residues, assignments were later confirmed by intra- and interresidue HN/C^{α} connectivities in 3D HNCA and HN(CO)CA experiments recorded with the doubly ^{13}C-/^{15}N-labelled VH. The remaining 12 residues could only be assigned with the help of the HNCA/HN(CO)CA data, as described in detail below.

Assignment was initiated on the basis of a ^{1}H-^{15}N HSQC spectrum (Fig. 1). Folded ^{1}H/^{15}N cross peaks were identified through variation of the spectral width in the ^{15}N dimension. Intraresidue cross peaks to these NH signals (Table 1) were extracted from a 3D TOCSY-HMQC spectrum. NH signals without at least a C^{α}H connectivity could mostly be identified as side-chain signals. However, for Cys^{92} an NH/H^{α} cross peak was observed in the homonuclear 2D TOCSY, but not in the 3D TOCSY-HMQC spectrum. Also in other cases cross peaks to well-separated NHs, which were observed in the homonuclear TOCSY recorded in H_2O, were used to complement spin systems. Furthermore, H^{α} and H^{β} cross peaks were cross-checked in a 2D DQF-COSY experiment recorded in D_2O, as signals above 3.9 ppm are undisturbed by the CHAPS signals. This proved especially helpful to distinguish some serine and glycine spin systems. Cross peaks to H^{α} signals with chemical shifts iden-

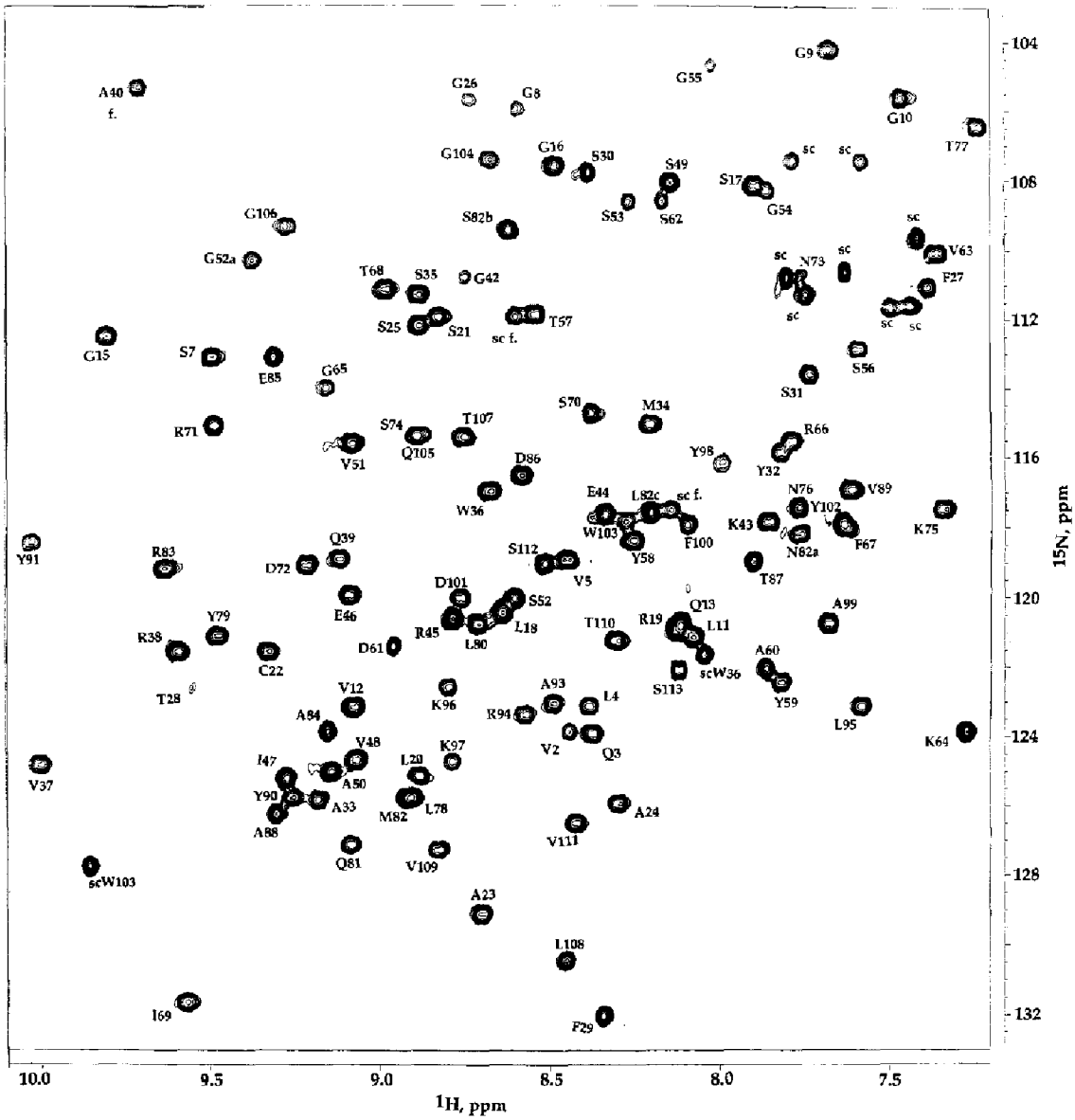

Fig. 1. ^1H-^{15}N HSQC spectrum of VH-P8. All backbone amides except Glu^6 and Cys^{92} are shown. Side-chain signals (sc, scW) are indicated.

tical to the water frequency at 303 K were distinguished from NH/H_2O exchange peaks by comparison with a 3D TOCSY-HMQC spectrum recorded at 313 K.

Spin systems were preliminarily sorted into valines, alanines, threonines, serines and glycines. Remaining spin systems were grouped into those with a H^β chemical shift larger (WYFCND) or smaller (EQMKRIL) than 2.5 ppm. At this stage it was clear that the number of observed signals corresponded roughly to that expected. Substantial overlap occurred only for the NH signals of Ser^{74}/Gln^{105} and Leu^{78}/Met^{82}, but was not problematic for the interpretation of the 3D spectra.

β-Strands

A 3D NOESY-HMQC experiment, recorded with a mixing time of 100 ms to minimise spin diffusion, was analysed for sequential $d_{\alpha N}(i,i+1)$ cross peaks. Because of the β-sheet arrangement typical for the immunoglobulin fold, $d_{\alpha N}(i,i+1)$ connectivities were expected to be most useful as a starting point for the sequential assignment. Indeed, numerous strong $d_{\alpha N}(i,i+1)$ cross peaks (Fig. 2) were observed and sequential assignments for stretches of two to five residues could be made. More complete assignments at this stage suffered from ambiguities due to the large number of β-strand residues, resulting in H^α chemical shift degeneracy. Analysis of d_{NN} cross peaks did not resolve these ambiguities, as most NH/NH cross peaks were clearly not sequential.

We refered instead to the well-known immunoglobulin β-sheet arrangement of nine β-strands (Fig. 3), which has been determined for VH domains in crystallographic studies of antibodies (Alzari et al., 1988; Colman, 1988). This seemed justified as the predominance of $d_{\alpha N}(i,i+1)$ cross peaks in the NOESY spectra, the H^α chemical shift

TABLE I
^{1}H, ^{15}N AND $^{13}C^{\alpha}$ ASSIGNMENTS OF VH-P8

Residue	Chemical shifts (ppm)							Relative difference[a]
	Free VH					Protein A-bound VH		
	HN	N	H^{α} (C^{α})	H^{β}	Others	HN	N	
Glu[1]			4.11 (53.3)	2.09				
Val[2]	8.45	123.8	4.10 (61.5)	0.77	H^{γ}_{3} 0.34, 0.06	8.45	123.8	< 0.2
Gln[3]	8.37	123.8	4.64 (53.3)	1.85, 1.93		8.37	123.8	< 0.2
Leu[4]	8.38	123.0	5.06 (51.6)	1.55		8.35	123.2	0.409
Val[5]	8.44	118.9	4.51 (60.0)	2.10	H^{γ}_{3} 1.02	8.44	118.9	< 0.2
Glu[6]	10.32	130.4	5.66 (55.2)	2.28		10.33	130.5	0.391
Ser[7]	9.49	113.1	4.82 (56.0)	3.94		9.49	113.2	0.143
Gly[8]	8.60	106.0	4.75, 3.79 (42.8)			8.56	105.9	0.279
Gly[9]	7.67	104.2	4.00, 3.57 (43.2)			7.67	104.2	< 0.2
Gly[10]	7.45	105.6	4.23, 3.94 (42.8)			7.36	105.6	0.873
Leu[11]	8.08	121.0	5.33 (52.2)	1.70, 1.50		8.08	121.0	< 0.2
Val[12]	9.08	123.1	4.54 (57.6)	1.95	H^{γ}_{3} 0.87	9.06	123.4	0.312
Gln[13]	8.12	120.7	4.79 (52.3)	1.93, 2.09	H^{γ} 2.49	8.11	120.2	0.467
Pro[14]	–	–	3.94 (61.6)	2.29, 1.96				
Gly[15]	9.80	112.5	4.45, 3.60 (42.9)			10.07	112.8	2.873
Gly[16]	8.48	107.6	4.34, 3.77 (42.5)			?	?	> 3
Ser[17]	7.90	108.1	5.61 (54.3)	3.83, 3.74		8.02	109.2	2.314
Leu[18]	8.64	120.4	4.41 (52.5)	1.33		?	?	> 3
Arg[19]	8.12	120.9	5.10 (52.3)	1.77	H^{γ} 1.38, H^{δ} 3.06	8.18	120.7	0.725
Leu[20]	8.89	125.0	4.96 (51.0)	0.82		8.89	125.0	< 0.2
Ser[21]	8.82	111.9	5.69 (54.9)	3.80, 3.71		?	?	> 3
Cys[22]	9.33	121.5	5.30 (51.4)	3.16, 2.89		9.20	121.1	1.458
Ala[23]	8.69	129.0	4.71 (49.0)	1.36		8.64	128.9	0.653
Ala[24]	8.30	125.9	5.42 (48.2)	1.01		8.30	125.9	< 0.2
Ser[25]	8.88	112.1	4.69 (55.3)	3.83		8.88	112.1	< 0.2
Gly[26]	8.74	105.8	4.53, 3.73 (43.4)			8.72	105.5	0.223
Phe[27]	7.38	111.0	5.15 (50.1)	3.04, 2.91	$H^{2,6}$ 7.08, $H^{3,5}$ 7.23, H^{4} 7.24	7.38	111.0	< 0.2
Thr[28]	9.55	122.5	4.27 (60.3)	4.45		9.55	122.5	< 0.2
Phe[29]	8.34	131.9	4.14 (58.9)		$H^{2,6}$ 6.89, $H^{3,5}$ 7.22, H^{4} 7.28	8.34	131.9	< 0.2
Ser[30]	8.39	107.7	3.93 (57.8)			8.37	107.6	0.221
Ser[31]	7.73	113.5	4.43 (57.2)	3.98, 3.77		7.74	113.8	0.322
Tyr[32]	7.82	115.8	4.75 (55.8)	3.23, 2.62	$H^{2,6}$ 7.51, $H^{3,5}$ 6.91	7.82	115.8	< 0.2
Ala[33]	9.18	125.7	4.45 (50.3)	1.40		9.16	125.9	0.263
Met[34]	8.21	114.9	5.51 (49.4)	1.51		8.16	115.1	0.335
Ser[35]	8.88	111.2	5.35 (54.9)	3.67		8.84	111.2	0.391
Trp[36]	8.67	116.9	5.80 (53.7)	3.15, 2.99	N^{1} 121.6, $H^{1}N$ 8.04, H^{2} 6.99, H^{4} 7.61, H^{5} 6.95, H^{6} 7.04, H^{7} 6.93	8.55	116.9	1.063
Val[37]	10.00	124.7	4.93 (58.1)	1.83	H^{γ}_{3} 0.84, 0.60	9.96	124.3	0.683
Arg[38]	9.58	121.5	6.04 (50.4)			9.53	121.2	0.743
Gln[39]	9.11	118.8	4.77 (52.9)	2.29		9.08	118.7	0.356
Ala[40]	9.72	135.4	4.87 (47.7)	1.48		9.72	135.4	< 0.2
Pro[41]	–	–	4.37 (62.1)					
Gly[42]	8.75	110.8	4.12, 3.79 (43.7)			8.68	110.9	0.726
Lys[43]	7.84	117.7	4.81 (52.1)	1.90	H^{γ} 1.38, H^{δ} 1.69, H^{ϵ} 3.08	7.84	117.7	< 0.2
Glu[44]	8.34	117.6	4.42 (53.7)	1.98		8.34	117.6	< 0.2
Arg[45]	8.78	120.6	4.52 (54.9)	1.68		8.75	120.5	0.294
Glu[46]	9.09	119.8	4.89 (52.1)	2.06	H^{γ} 2.26	9.08	120.2	0.316
Ile[47]	9.28	125.2	4.20 (61.2)	2.08	H^{γ}_{3} 1.04	9.19	125.2	0.687
Val[48]	9.07	124.7	4.33 (61.6)	2.34	H^{γ}_{3} 1.28, 1.24	8.99	124.3	0.954
Ser[49]	8.14	107.9	5.47 (54.1)	4.09, 3.77		8.10	107.4	0.912
Ala[50]	9.14	124.9	5.33 (49.9)	1.43		9.08	125.3	0.809
Val[51]	9.08	115.5	5.35 (56.5)	2.12	H^{γ}_{3} 0.91	9.02	115.3	0.695
Ser[52]	8.61	119.9	4.25 (56.0)			8.53	119.9	0.642
Gly[52a]	9.38	110.4	3.75, 3.28 (46.0)			9.38	110.6	0.429
Ser[53]	8.28	108.6	4.26 (56.8)			8.28	108.6	< 0.2
Gly[54]	7.86	108.2	4.48, 3.52 (42.4)			7.88	108.2	0.350
Gly[55]	8.03	104.7	4.04, 3.87 (44.2)			8.02	104.3	0.426
Ser[56]	7.59	112.7	5.13 (55.4)	3.89, 3.63		7.48	112.4	1.393
Thr[57]	8.54	111.8	5.26 (57.5)	3.97	H^{γ}_{3} 1.29	8.39	112.3	1.602
Tyr[58]	8.25	118.3	4.84 (54.5)	2.31, 3.08	$H^{2,6}$ 6.82, $H^{3,5}$ 6.69	8.18	118.7	0.978
Tyr[59]	7.82	122.3	4.69 (54.9)	2.35, 2.85	$H^{2,6}$ 7.11, $H^{3,5}$ 6.88	7.71	122.1	1.178
Ala[60]	7.86	122.0	4.32 (50.0)	1.75		7.82	122.2	0.409

TABLE 1 (continued)

Residue	Chemical shifts (ppm)							Relative difference[a]
	Free VH					Protein A-bound VH		
	HN	N	H^{α} (C^{α})	H^{β}	Others	HN	N	
Asp^{61}	8.96	121.3	4.26 (56.0)	2.74		8.93	121.3	0.246
Ser^{62}	8.17	108.6	4.22 (57.6)			8.16	108.7	0.222
Val^{63}	7.35	110.0	4.19 (58.1)	1.14	H^{γ}_3 1.08, 0.30	7.25	109.7	1.258
Lys^{64}	7.26	123.8	3.69 (56.4)	1.81	H^{γ} 1.44	7.28	124.6	0.981
Gly^{65}	9.16	114.0	4.31, 3.58 (43.3)			?	?	>3
Arg^{66}	7.78	115.4	4.64 (55.1)	1.68		?	?	>3
Phe^{67}	7.62	118.0	6.15 (50.5)	3.07	$H^{2,6}$ 7.13, $H^{3,5}$ 7.35, H^{4} 7.15	?	?	>3
Thr^{68}	8.98	111.1	5.22 (59.4)	3.91	H^{γ}_3 1.28	?	?	>3
Ile^{69}	9.57	131.6	5.40 (57.3)			?	?	>3
Ser^{70}	8.37	114.6	4.79 (55.7)	4.09		?	?	>3
Arg^{71}	9.49	115.0	5.54 (52.2)			?	?	>3
Asp^{72}	9.21	118.9	5.16 (50.0)	3.13, 2.72		9.24	119.1	0.445
Asn^{73}	7.78	110.4	5.16 (53.1)			7.74	110.8	0.205
Ser^{74}	8.87	115.3	4.62 (58.6)	4.12, 4.06		8.81	115.3	0.466
Lys^{75}	7.33	117.4	4.52 (53.0)	1.42		7.36	117.6	0.480
Asn^{76}	7.76	117.4	3.39 (51.9)	2.82, 2.66		7.76	117.1	0.277
Thr^{77}	7.23	106.4	5.15 (58.6)	3.43	H^{γ}_3 0.62	7.27	106.2	0.546
Leu^{78}	8.89	125.6	4.99 (51.0)	1.93		?	?	>3
Tyr^{79}	9.47	121.0	5.95 (55.1)	3.04	$H^{2,6}$ 7.05, $H^{3,5}$ 6.74	9.37	120.3	1.597
Leu^{80}	8.71	120.7	4.75 (52.1)		H^{δ}_3 0.76, −0.38	?	?	>3
Gln^{81}	9.08	127.0	4.35 (52.7)	2.08	H^{γ} 2.46	9.36	127.3	2.788
Met^{82}	8.91	125.7	4.07 (52.8)	1.77		?	?	>3
Asn^{82a}	7.76	118.1	5.22 (49.0)	3.19, 2.82		?	?	>3
Ser^{82b}	8.62	109.4	3.70 (55.5)	4.09, 3.76		8.57	108.7	1.036
Leu^{82c}	8.20	117.5	4.02 (54.8)	1.53		?	?	>3
Arg^{83}	9.63	119.1	4.82 (51.7)	1.69		9.63	119.1	<0.2
Ala^{84}	9.15	123.8	4.17 (54.0)	1.54		9.11	123.6	0.393
Glu^{85}	9.31	113.0	4.37 (56.4)	2.28, 2.11		9.19	113.1	0.953
Asp^{86}	8.58	116.4	4.84 (52.9)	3.12, 2.86		8.58	116.3	0.204
Thr^{87}	7.90	118.9	4.60 (62.6)	4.40	H^{γ}_3 1.58	7.90	118.9	<0.2
Ala^{88}	9.30	126.1	4.42 (50.5)	1.18		9.21	126.2	0.775
Val^{89}	7.60	116.9	4.39 (61.0)	1.96	H^{γ}_3 1.00, 0.42	7.57	116.9	0.316
Tyr^{90}	9.25	125.8	4.87 (56.1)	3.02, 2.64	$H^{2,6}$ 7.10, $H^{3,5}$ 6.98	9.21	125.8	0.484
Tyr^{91}	10.02	118.4	5.23 (54.2)	2.96, 2.88	$H^{2,6}$ 7.01, $H^{3,5}$ 6.56	9.96	118.5	0.666
Cys^{92}	11.03	123.3	4.51 (51.2)	3.13, 2.97		11.03	123.3	<0.2
Ala^{93}	8.49	123.0	4.94 (49.0)	0.46		8.49	123.0	<0.2
Arg^{94}	8.58	123.3	5.00 (53.3)	2.30		8.54	123.3	0.211
Leu^{95}	7.58	123.1	4.68 (52.2)	1.41		7.60	123.2	0.391
Lys^{96}	8.80	122.5	4.36 (54.1)	1.67		8.80	122.5	<0.2
Lys^{97}	8.77	124.7	3.49 (56.8)	1.82, 1.75		8.76	124.6	0.240
Tyr^{98}	7.99	116.2	4.45 (54.5)	3.23, 2.93	$H^{2,6}$ 7.06, $H^{3,5}$ 6.84	7.99	116.2	<0.2
Ala^{99}	7.68	120.7	4.38 (48.2)	1.36		7.68	120.7	<0.2
Phe^{100}	8.10	117.9	5.34 (54.3)	2.89, 2.56	$H^{2,6}$ 6.98, $H^{3,5}$ 7.10, H^{4} 6.92	8.04	117.8	0.485
Asp^{101}	8.76	119.9	4.66 (51.9)	2.53, 2.42		8.76	119.9	<0.2
Tyr^{102}	7.62	117.7	4.40 (56.7)	2.72, 2.11	$H^{2,6}$ 6.87, $H^{3,5}$ 6.70	7.60	117.9	0.437
Trp^{103}	8.27	117.7	5.28 (54.3)	3.46, 2.95	N^{1} 127.7, $H^{1}N$ 9.86, H^{2} 7.25, H^{4} 7.24, H^{5} 6.68, H^{6} 6.44, H^{7} 7.02	8.23	117.8	0.299
Gly^{104}	8.67	107.4	4.94, 4.69 (43.4)			8.60	107.4	0.631
Gln^{105}	8.89	115.3	4.62 (54.9)	2.35		8.89	115.3	<0.2
Gly^{106}	9.27	109.3	3.51 (42.0)			9.30	109.3	0.340
Thr^{107}	8.74	115.4	4.79 (58.0)	3.89	H^{γ}_3 1.22	8.69	115.2	0.605
Leu^{108}	8.45	130.4	4.65 (54.0)	1.85		8.45	130.4	<0.2
Val^{109}	8.83	127.2	4.44 (60.0)	2.40	H^{γ}_3 0.63	8.83	127.2	<0.2
Thr^{110}	8.30	121.2	4.59 (59.5)	3.91	H^{γ}_3 1.15	8.20	121.1	0.959
Val^{111}	8.42	126.4	4.89 (57.8)	1.96	H^{γ}_3 0.69, 0.46	8.42	126.4	<0.2
Ser^{112}	8.51	118.9	4.53 (55.7)	3.78, 3.66		8.52	119.4	0.517
Ser^{113}	8.13	122.1	4.36 (58.4)	3.92		8.07	121.9	0.455

Chemical shifts were determined from experiments recorded at 303 K and pH 6.2. Question marks for the HN and N signals of the Protein A-bound VH residues indicate that their unambiguous assignment was impossible.

[a] The relative difference between chemical shifts determined for resonances of free VH and of VH complexed with the IgG-binding fragment of Protein A were calculated as the sum of the ^{1}H and ^{15}N chemical shift differences. The ^{1}H chemical shift differences were multiplied by 9 to adjust for the smaller ^{1}H chemical shift dispersion. Differences are computed using non-rounded chemical shifts and can therefore vary from differences of rounded values shown in the table.

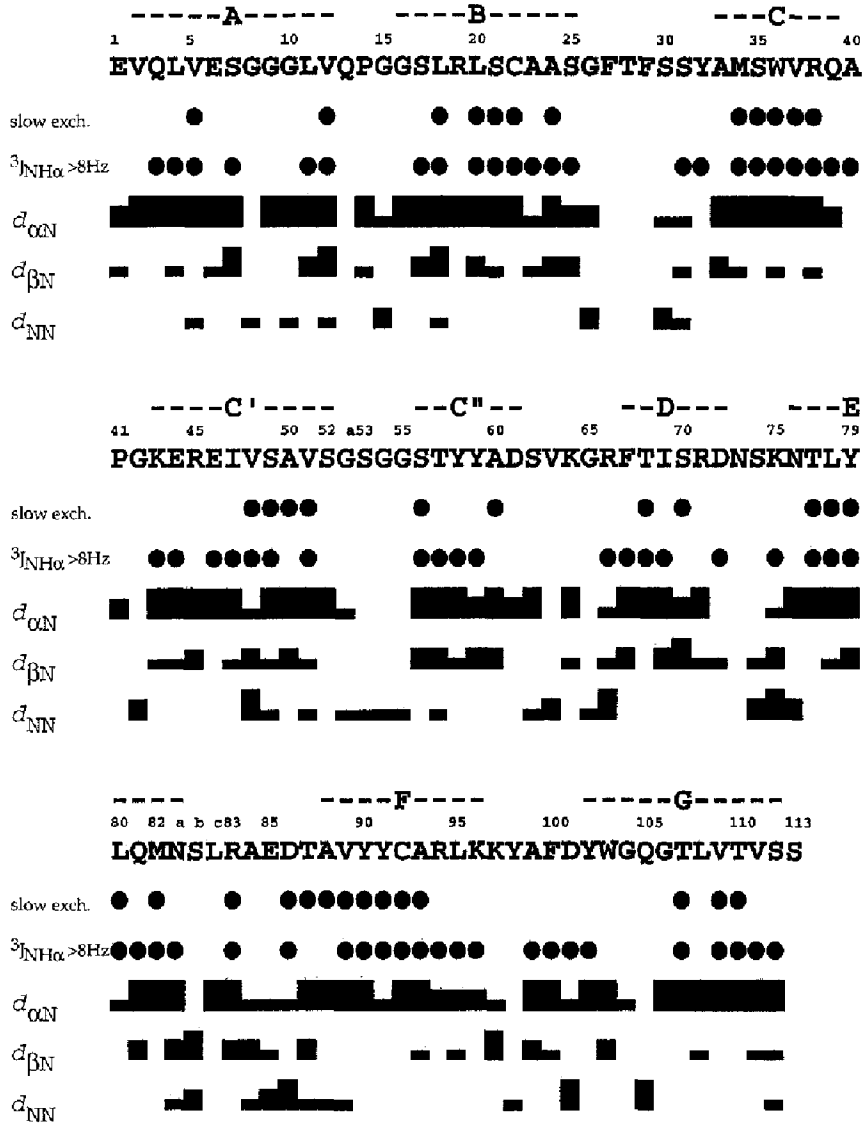

Fig. 2. Primary sequence of VH-P8 with d(i,i+1) NOEs. NOEs were observed in the 3D NOESY-HMQC spectrum (τ_m=100 ms) recorded at 303 K. Medium-range NOEs like d(i,i+2) etc. are discussed in the text. Residues are numbered according to Kabat et al. (1991). NOE intensities are shown with different bar sizes, according to their integrated volumes as strong, medium or weak. β-Strands are labelled following the nomenclature of Colman (1988).

values and the slow exchange in D_2O observed for many of the involved amides suggested the overwhelming presence of β-structure. A schematic diagram of the backbone arrangement of residues within the expected β-sheets in VH-P8 (Fig. 3) indicated numerous interstrand NH/NH and H^{α}/H^{α} interactions. Many of these were indeed found (Fig. 3) in the 3D NOESY-HMQC or 2D NOESY spectrum recorded in D_2O and allowed identification of the β-strands. The assignment of all residues forming β-structure was confirmed later by their $^{13}C^{\alpha}$ cross peaks in the HNCA/HN(CO)CA spectra (Fig. 4).

The β-strands were interrupted between Glu^{46} and Ser^{49} in strand C' and between Gly^{104} and Thr^{107} in strand G (Fig. 2). At these positions, β-bulges have been described in crystallographically solved VH structures. Strong sequential $d_{NN}(i,i+1)$ NOEs between Val^{48} and Ser^{49} and between Gln^{105} and Gly^{106}, as well as weak $d_{\alpha N}(i,i+1)$ cross peaks between the other residues involved (Fig. 2), enabled assignment in these regions. The β-structure in strand A was interrupted between Ser^{7} and Gly^{10}. Residues Gly^{8} and Gly^{9} could not be assigned without the HNCA/HN(CO)CA data, due to lack of NOEs.

Turns and loops

Assignment of the turn around residue Pro^{14}, which connects β-strands A and B, was based on $d_{\alpha N}$ and d_{NN} NOEs observed between Gln^{13} and Gly^{16} and their respective neighbours in the primary sequence. In the other proline-containing (Pro^{41}) turn, that between strands C and C', Gly^{42} was assigned based on a $d_{NN}(i,i+1)$ cross peak to Lys^{43}. Residue Ala^{40} was assigned through a $d_{\alpha N}(i,i+1)$ cross peak from Gln^{39}.

Residues 62 to 66, which connect strands C" and D, exhibit no distinct secondary structure. Strong to medium

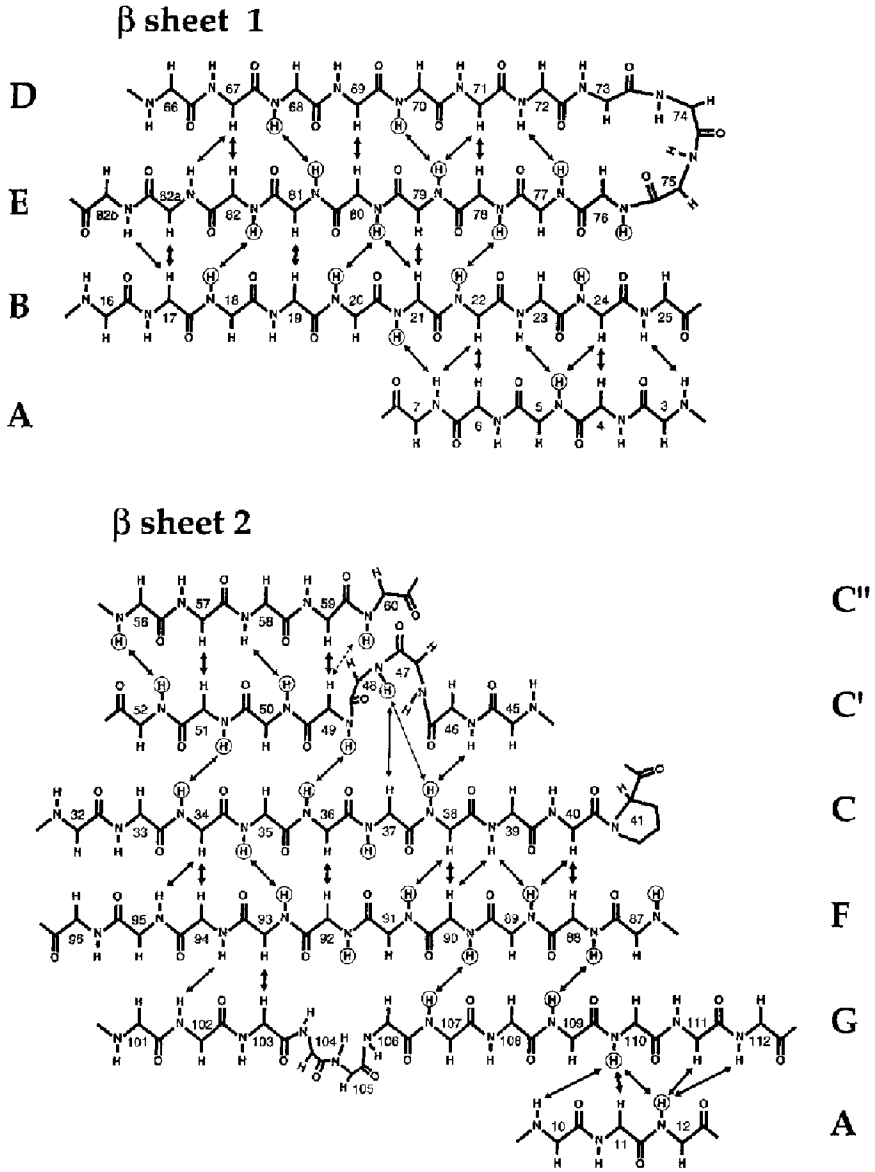

Fig. 3. Schematic diagram of the β-strand arrangement in VH-P8. Interstrand main-chain NOEs identified in 3D NOESY-HMQC and 2D NOESY experiments recorded in D_2O at 303 K are indicated by arrows (different arrow types are for drawing convenience and do not reflect NOE intensities).

$d_{NN}(i,i+1)$ and $d_{\alpha N}(i,i+1)$ cross peaks alternate in this region and facilitated assignment. The turn between strands D and E is formed by residues 73 to 76. For residues Ser^{74}, Lys^{75} and Asn^{76}, sequential $d_{NN}(i,i+1)$ cross peaks were observed. For Asn^{73}, neither NOE nor HNCA or HN(CO)CA cross peaks and only a weak $^1H/^{15}N$ cross peak (Fig. 1) were observed, probably due to exchange. Asn^{73} was finally assigned through exclusion. The β-strands E and F are connected by residues 82c to 87. Throughout this region sequential $d_{\beta N}$ and/or $d_{\alpha N}(i,i+1)$ NOEs were present, which, together with strong sequential $d_{NN}(i,i+1)$ cross peaks between Ser^{82b} and Leu^{82c} and between Asp^{86} and Thr^{87}, enabled assignment (see Fig. 2).

Concerning the assignment of the hypervariable loops 1 to 3 in their respective CDRs, the ^{15}N-resolved data were only sufficient to assign hypervariable loop H3 within CDR3, which links β-strands F and G. Residues within H3 were assigned through several (i,i+1) NOEs (Fig. 2), further supported by $d_{NN}(i,i+3)$ NOEs between Lys^{96} and Ala^{99} and between Ala^{99} and Tyr^{102}. The remaining two loops H1 and H2 in CDRs 1 and 2 were only sequentially assigned with the help of the $HN/^{13}C^{\alpha}$ cross peaks from the HNCA and HN(CO)CA experiments.

In loop H1 of CDR1, the last three residues (Ser^{30}, Ser^{31} and Tyr^{32}) exhibit both $d_{\alpha N}$ and d_{NN} (i,i+1) NOEs. For Ser^{25}, $d_{\alpha N}$ and $d_{\beta N}$ NOEs to both Gly^{26} and Phe^{27} were observed. However, as for both Thr^{28} and Phe^{29} neither H^{β} cross peaks in the TOCSY nor sequential $d_{\alpha N}$ and d_{NN} NOEs in the NOESY experiments were seen,

assignment of the complete H1 loop became only evident from the HNCA/HN(CO)CA experiments.

The H2 loop presented a particular problem, as it consists of three glycines (Gly^{52a}, Gly^{54} and Gly^{55}) and one serine (Ser^{53}), for all of which only weak NOEs were observed (Fig. 2). Thus, their sequential assignment and even their distinction from Gly^{8} and Gly^{9} were only possible on the basis of $^{13}C^{\alpha}$ data.

Structure

The overwhelming structural element in the VH is the β-strand. This is indicated by the relative intensities of $d_{\alpha N}(i,i+1)$ NOEs compared to intraresidue NH/H^{α} or $d_{NN}(i,i+1)$ NOEs (Fig. 2). Also, most residues with a strong $d_{\alpha N}(i,i+1)$ NOE (Fig. 2) and indeed most residues of the entire VH (66 out of the 114 observable backbone amides) have a $^{3}J_{NHC\alpha H}$ coupling constant larger than 8 Hz, typical for β-structure. Both at 303 K and at 313 K, 37 backbone amide protons were protected from D_2O exchange, suggesting a high stability of the VH domain. Of the slowly exchanging amide protons, 32 have a large $^{3}J_{NHC\alpha H}$ coupling constant (Fig. 2), indicating sheet formation of the β-strands with an extensive hydrogen bond network. Indeed, 23 long-range NH/NH, 13 long-range NH/H^{α} and 15 long-range H^{α}/H^{α} NOEs were identified, in agreement with formation of two β-sheets comprising (with one small exception) antiparallel oriented β-strands typical for immunoglobulin variable domains (Fig. 3). The general β-sheet arrangement of the VH, including their β-bulges, is indeed identical to that found in crystal structures of VL-associated VH domains as part of Fab fragments (Alzari et al., 1988; Colman, 1988). The sheets are depicted in Fig. 3 and the connecting turns and loops have been discussed above.

VL interface

Whereas there are no discrepancies between the general β-arrangement of VH domains in solved crystal structures of antibodies and the isolated VH, differences are more likely to occur in its VL interface. This interface should be exposed to the solvent, as gel filtration indicates formation of only monomeric VH. In intact immunoglobulins, the VL interface of a VH is mostly formed by β-sheet 2 (Poljak et al., 1975; Chothia et al., 1985). Within this sheet, the highly conserved VH residues 45, 47 and 103 have most of their accessible surface area buried in the interface. These residues are located around two interruptions of β-structure found in strands C' and G in VH-P8, which coincide with the β-bulges in crystal VH structures as part of Fabs or Fvs. Thus, the main-chain structure of even the former VL interface of the isolated VH is very similar to that in a light chain-associated VH.

However, three mutations (G44E, L45R and W47I) had been introduced in VH-P8 to improve its NMR line width from 16 to 11 Hz when wild-type VH and VH-P8 were compared in the presence of the detergent CHAPS (Davies and Riechmann, 1994). Two of these residues, 45 and 47, are among those contributing most of their surface area to the VH/VL interface. Despite the lack of differences to the secondary structure of VH domains in intact antibodies, mutational analysis indicates that changes in the isolated VH go beyond a simple increase of the surface hydrophilicity due to the different character of solvent-exposed side chains. Thus, with respect to residue 47, the nature of its side chain does not only affect solubility and NMR line width, but also stability. Two engineered mutants of VH-P8, in which Ile^{47} was replaced by either glycine (reported for several camelid VHs (Muyldermans et al., 1994)), or serine, are less stable

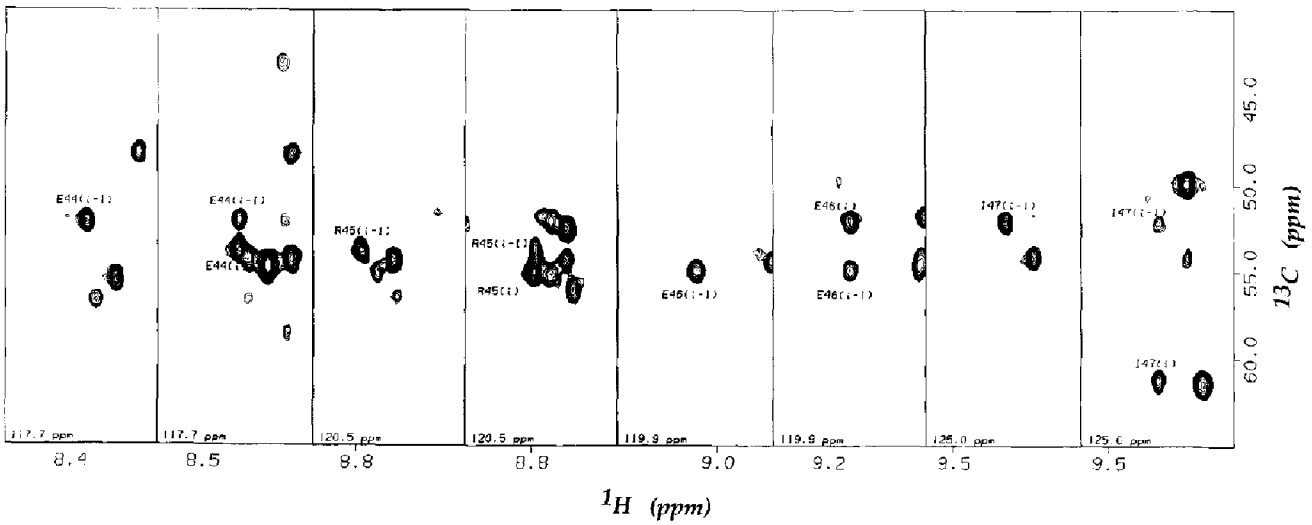

Fig. 4. Amide strips taken from 3D HNCA and HN(CO)CA experiments recorded with ^{15}N-/^{13}C-labelled VH-P8. Interresidue [(i−1) in HNCA and HN(CO)CA] and intraresidue [(i) in HNCA] NH/C^{α} cross peaks for residues Glu^{44} to Ile^{47} and the amide ^{15}N frequency are shown in strips taken from the respective 3D spectra.

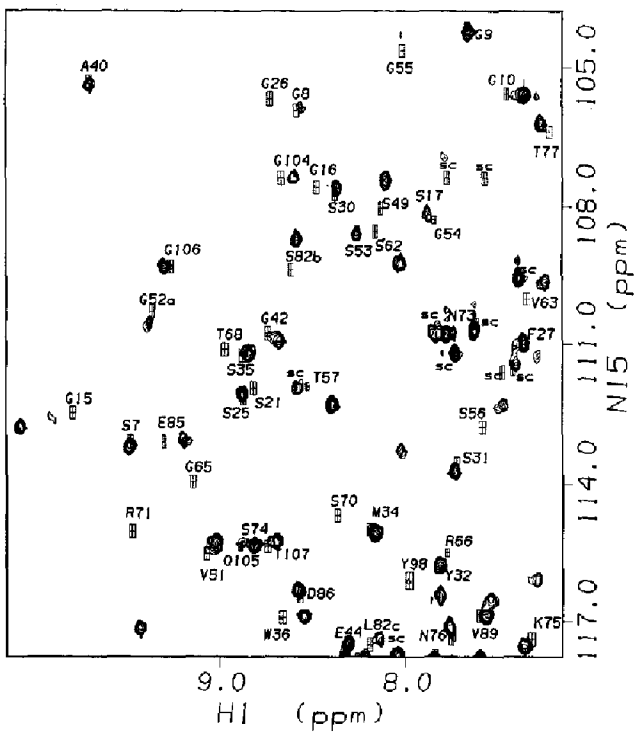

Fig. 5. ^{1}H-^{15}N HSQC spectrum of the complex of VH-P8 and the IgG-binding fragment of Protein A. Locations of amide signals observed for the free VH-P8 (see Fig. 1) are indicated.

than VH-P8 (Davies and Riechmann, 1994). Thus, their amide protons were all exchanged in D_2O after 1 h at 303 K and most protein precipitated fast in the NMR tube, although the remaining soluble protein showed 2D spectra that were very similar to those recorded with VH-P8.

The importance of residue 47 for the stability of an isolated VH is surprising, as in intact antibodies it is a highly conserved tryptophan (Kabat et al., 1991) central in the VL interface (Chothia et al., 1985). The role of residue 47 in isolated VH domains should become obvious from a detailed tertiary structure.

Protein A binding

The isolated VH domain VH-P8 originates from the VH gene DP-47, which is a member of the human VH_{III} subgroup of genes (Tomlinson et al., 1992). Antibodies containing a VH belonging to this subgroup bind Protein A independent of the subclass of their constant region (Sasso et al., 1991). Their binding site resides in the heavy chain variable domain and not (only) in the Fc portion like another, more commonly known Protein A binding site of many Ig isotypes (Langone, 1982). As Protein A sepharose is an efficient and widely used reagent to purify intact antibodies, its use for the purification of antibody fragments lacking an Fc portion has great attraction. Knowledge of the location of the Protein A binding site in the human VH_{III} subgroup might enable the design of such a binding site in VH domains originating from other VH genes.

To study the interactions of Protein A with VH-P8, the ^{15}N-enriched VH was complexed with the secreted form of *S. aureus* Protein A (41 kDa) or its recombinant IgG-binding fragment (15 kDa). Binding to the complete Protein A increased the line width of the VH so dramatically that the detection of most $^{1}H/^{15}N$ cross peaks in a ^{1}H-^{15}N HSQC experiment was impossible. The line width of the VH signals also increased (as expected from the increase in molecular weight) when complexed with the IgG-binding fragment of Protein A. However, all $^{1}H/^{15}N$ amide signals could still be observed in a ^{1}H-^{15}N HSQC experiment (Fig. 5). The chemical shifts of many residues were altered, showing that the IgG-binding fragment of Protein A binds to the VH. Thus, the binding sites on Protein A for the Fc portion of IgG and for the variable domains of the human VH_{III} subgroup are both located

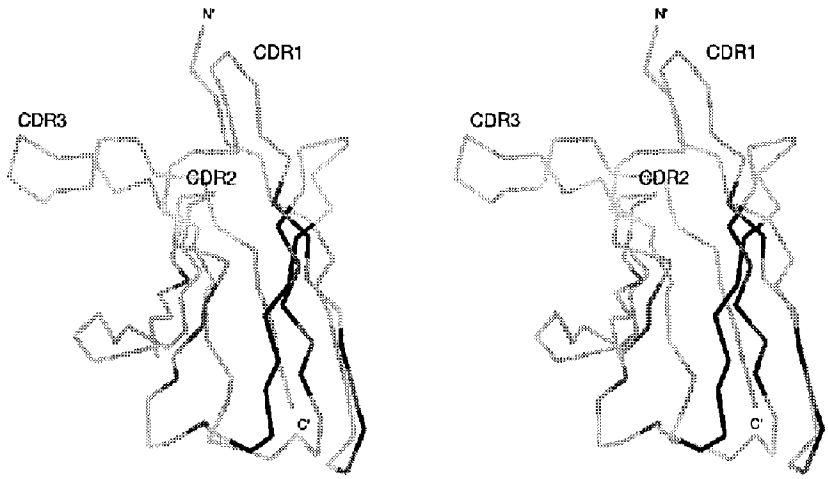

Fig. 6. Backbone trace of a modelled VH domain (McManus and Riechmann, 1991). Residues, whose amide chemical shift could not be identified in the ^{1}H-^{15}N HSQC spectrum of VH-P8 after addition of the IgG-binding fragment of Protein A, are shown in black. Among the identified residues, those with the 10 biggest chemical shift changes upon binding are shown in dark grey.

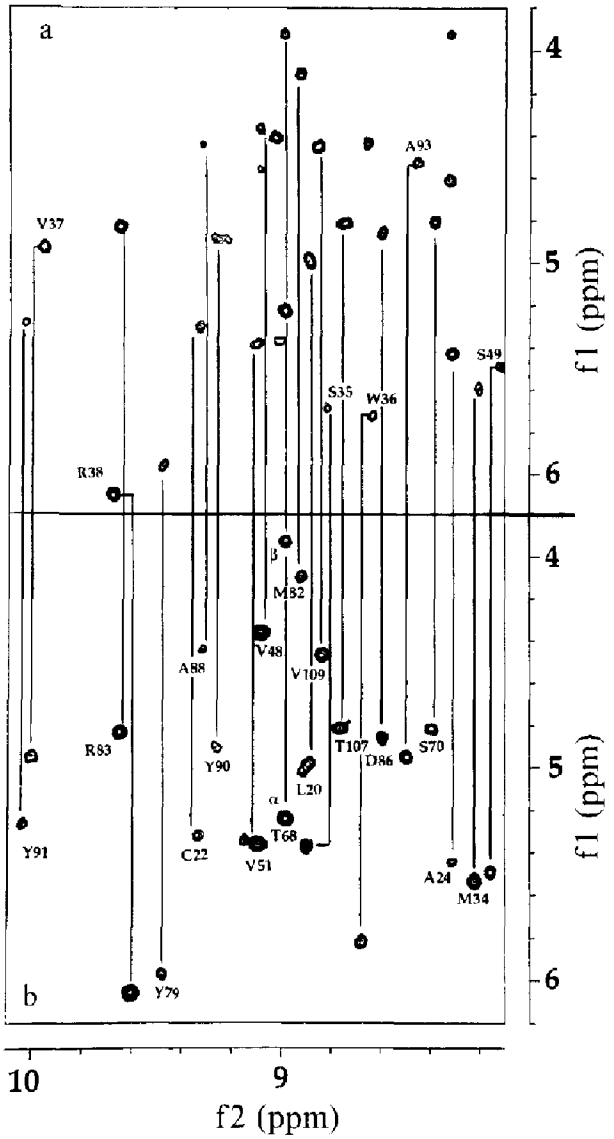

Fig. 7. 2D TOCSY spectra of (a) VH-Ox21 and (b) VH-P8. Cross peaks are labelled in (a) unless chemical shift differences between VH-Ox21 and VH-P8 are observed, in which case they are labelled in (b). Spectra were recorded in D_2O with a mixing time of 50 ms.

in the IgG-binding fragment of Protein A. This is not surprising, as this fragment (residues 60 to 186 of the mature Protein A) comprises two of the five homologous repeat units, each of which has a binding site for IgG (Langone, 1982; Uhlen et al., 1984).

Most residues in the VH encounter only minor chemical shift changes after binding to the IgG-binding fragment (Fig. 5 and Table 1), enabling their preliminary assignment. However, 15 VH residues could not be assigned and for several others significant changes are observed. Most of these residues reside in sheet 1 (strands B, D and E) of the VH. This sheet lies opposite the natural VL interface. Both in the VH and in intact antibodies, one side of sheet 1 is exposed to the solvent and therefore accessible for intermolecular interactions.

We propose that Protein A binding takes place through the VH surface formed by β-sheet 1 (Fig. 6). This corroborates a prediction based on the location of the most subgroup-specific residues in members of the VH_{III} subgroup of genes, according to which the Protein A binding site involves residues 6 to 24 and 67 to 85 (Sasso et al., 1991). Changes observed for residues in the outer strand C" of sheet 2 indicate that the binding site might also extend to the edge of the second sheet. However, long-range conformational changes outside the Protein A binding site might account especially for the perturbance of signals originating from residues not located in sheet 1. Thus, the chemical shift change observed for residue 36 in sheet 2 is likely to be due to indirect effects. In intact antibodies, the side chain of residue Trp^{36} is buried between the two sheets and its side chain amide shift is indeed more strongly affected by Protein A binding than the backbone amide shift.

The large chemical shift changes seen for many residues in sheet 1 of the VH contrast the only minor effects of Protein A binding on residues in the hypervariable loops. This explains why randomisation of residues in the hypervariable loops to create antigen-binding Fv fragments (Hoogenboom and Winter, 1992) or VH domains (Davies and Riechmann, 1995) does not affect Protein A binding.

Conclusions

Modifications in its VL interface, combined with the addition of detergent, enables the complete NMR analysis of an isolated immunoglobulin VH domain. This can include studies of backbone dynamics and structure determination after assignment of the ^1H and ^{13}C resonances and ^{15}N-/^{13}C-correlated NOE analysis, as already performed on an immunoglobulin VL domain (Constantine et al., 1992,1993a,b,1994). As the VH originates from the most frequently utilised human VH gene (DP-47) (Griffiths et al., 1994), its analysis can also aid that of many human Fv fragments. However, NMR line width and solubility of such Fv fragments are comparable (J. Davies and L. Riechmann, unpublished results) to that of other Fvs studied (Riechmann et al., 1991; Takahashi et al., 1992; Goldfarb et al., 1993; Freund et al., 1994), making an NMR analysis difficult.

The NMR analysis of other VH domains will be simpler. After antigen selection of a phage-displayed library, VH domains specific for hapten, protein and peptide ligands have been selected (Davies and Riechmann, 1995; L. Riechmann, unpublished results). These VH domains are identical to VH-P8 except for the third hypervariable loop. Their assignment can be based on that of VH-P8. This was demonstrated for one of the selected VH domains (VH-Ox21), which binds the hapten 4-glycyl-2-phenyloxazol-5-one with good affinity (K_d = 186 nM). The stability and expression of VH-Ox21 are similar to those

of VH-P8. Despite the considerably longer H3 loop of VH-Ox21 (15 instead of 8 residues in VH-P8), most non-exchanging protons within the β-sheets give virtually superimposable NH/H^{α} cross peaks in a homonuclear 2D TOCSY experiment in D_2O when compared with VH-P8.

The favourable biochemical properties of the studied VH domains suggest that these antibody fragments can become powerful building blocks for the design of minimum recognition units and their further improvement will benefit from the structural analysis presented here.

Acknowledgements

J.D. receives a Medical Research Council studentship.

References

Alzari, P.M., Lascombe, M.-B. and Poljak, R.J. (1988) *Annu. Rev. Immunol.*, **6**, 555–580.

Anglister, J., Grzesiek, S., Ren, H., Klee, C.B. and Bax, A. (1993) *J. Biomol. NMR*, **3**, 121–126.

Bax, A., Clore, G.M., Driscoll, P.C., Gronenborn, A.M., Ikura, M. and Kay, L.E. (1990a) *J. Magn. Reson.*, **87**, 620–627.

Bax, A., Clore, G.M. and Gronenborn, A.M. (1990b) *J. Magn. Reson.*, **88**, 425–431.

Bodenhausen, G. and Ruben, D.J. (1980) *Chem. Phys. Lett.*, **69**, 185–188.

Braunschweiler, L. and Ernst, R.R. (1983) *J. Magn. Reson.*, **53**, 521–528.

Cavanagh, J. and Rance, M. (1992) *J. Magn. Reson.*, **96**, 670–678.

Chothia, C., Novotny, J., Bruccoleri, R. and Karplus, M. (1985) *J. Mol. Biol.*, **186**, 651–663.

Clore, G.M. and Gronenborn, A. (1991) *Science*, **252**, 1390–1399.

Colcher, D., Bird, R., Roselli, M., Hardman, K.D., Johnson, S., Pope, S., Dodd, S.W., Pantoliano, M.W., Milenic, D.E. and Schlom, J. (1990) *J. Natl. Cancer Inst.*, **82**, 1191–1197.

Colman, P.M. (1988) *Adv. Immunol.*, **43**, 99–132.

Constantine, K.L., Goldfarb, V., Wittekind, M., Anthony, J., Ng, S.-C. and Mueller, L. (1992) *Biochemistry*, **31**, 5033–5043.

Constantine, K.L., Friedrichs, M.S., Goldfarb, V., Jeffrey, P.D., Sheriff, S. and Mueller, L. (1993a) *Protein Struct. Funct. Genet.*, **15**, 290–311.

Constantine, K.L., Goldfarb, V., Wittekind, M., Friedrichs, M.S., Anthony, J., Ng, S.-C. and Mueller, L. (1993b) *J. Biomol. NMR*, **3**, 41–54.

Constantine, K.L., Friedrichs, M.S., Metzler, W.J., Hensley, P. and Mueller, L. (1994) *J. Mol. Biol.*, **236**, 310–327.

Davies, J. and Riechmann, L. (1994) *FEBS Lett.*, **339**, 285–290.

Davies, J. and Riechmann, L. (1995) *Biotechnology*, **13**, 475–479.

Farmer, B.T., Venters, R.A., Spicer, L.D., Wittekind, M.G. and Müller, L. (1992) *J. Biomol. NMR*, **2**, 195–202.

Freund, C., Ross, A., Plückthun, A. and Holak, T.A. (1994) *Biochemistry*, **33**, 3296–3303.

Goldfarb, V., Wittekind, M., Jeffrey, P.D., Mueller, L. and Constantine, K.L. (1993) *J. Mol. Biol.*, **232**, 15–22.

Griffiths, A.D., Williams, S.C., Hartley, O., Tomlinson, I.M., Waterhouse, P., Crosby, W.L., Kontermann, R.E., Jones, P.T., Low, N.M., Allison, T.J., Prospero, T.D., Hoogenboom, H., Nissim, A., Cox, J.P.L., Harrison, J.L., Zaccolo, M., Gheradi, E. and Winter, G. (1994) *EMBO J.*, **13**, 3245–3260.

Grzesiek, S. and Bax, A. (1992) *J. Magn. Reson.*, **96**, 432–440.

Grzesiek, S., Anglister, J. and Bax, A. (1993) *J. Magn. Reson. Ser. B*, **101**, 114–119.

Hamers-Casterman, C., Atarhouch, T., Muyldermans, S., Robinson, G., Hamers, C., Bajyana Songa, E., Bendahman, N. and Hamers, R. (1993) *Nature*, **363**, 446–448.

Harber, E. and Richards, F.F. (1966) *Proc. R. Soc. London B*, **166**, 176–187.

Hoogenboom, H.R. and Winter, G. (1992) *J. Mol. Biol.*, **227**, 381–388.

Jaton, J.-C., Klinman, N.R., Givol, D. and Sela, M. (1968) *Biochemistry*, **7**, 4185–4195.

Jeener, J., Meier, B.H., Bachmann, P. and Ernst, R.R. (1979) *J. Chem. Phys.*, **71**, 4546–4553.

Kabat, E.A., Wu, T.T., Perry, H.M., Gottesmann, K.S. and Foeller, C. (1991) *Sequences of Immunological Interest*, 5th ed., US Department of Health and Human Services, Washington, DC.

Kay, L.E. and Bax, A. (1990) *J. Magn. Reson.*, **86**, 110–126.

Köhler, G. and Milstein, C. (1975) *Nature*, **256**, 495–497.

Langone, J.J. (1982) *Adv. Immunol.*, **32**, 157–252.

Live, D.H., David, D.G., Agosta, W.C. and Cowburn, D. (1984) *J. Am. Chem. Soc.*, **106**, 1939–1941.

Marion, D. and Wüthrich, K. (1983) *Biochem. Biophys. Res. Commun.*, **113**, 967–974.

McManus, S. and Riechmann, L. (1991) *Biochemistry*, **30**, 5851–5857.

Messerle, B.A., Wider, G., Otting, G., Weber, C. and Wüthrich, K. (1989) *J. Magn. Reson.*, **85**, 608–613.

Muyldermans, S., Atarhouch, T., Saldanha, J., Barbosa, J.A.R.G. and Hamers, R. (1994) *Protein Eng.*, **7**, 1129–1135.

Nedelman, M.A., Shealy, D.J., Boulin, R., Brunt, E., Seasholtz, J.I., Allen, I.E., McCartney, J.E., Warren, F.D., Oppermann, H., Pang, R.H.L., Berger, H.J. and Weisman, H.F. (1993) *J. Nucl. Med.*, **34**, 234–241.

Poljak, R.J., Amzel, L.M., Chen, B.L., Phizackerley, R.P. and Saul, F. (1975) *Immunogenetics*, **2**, 393–394.

Rance, M., Sørensen, O.W., Bodenhausen, G., Wagner, G. and Ernst, R.R. (1983) *Biochem. Biophys. Res. Commun.*, **117**, 479–485.

Riechmann, L., Foote, J. and Winter, G. (1988) *J. Mol. Biol.*, **203**, 825–828.

Riechmann, L., Cavanagh, J. and McManus, S. (1991) *FEBS Lett.*, **287**, 185–188.

Rockey, J.H. (1967) *J. Exp. Med.*, **125**, 249–275.

Sandhu, J.S. (1992) *Crit. Rev. Biotechnol.*, **12**, 437–462.

Sasso, E.H., Silvermann, G.J. and Mannick, M. (1991) *J. Immunol.*, **147**, 1877–1883.

Shaka, A.J., Barker, P.B. and Freeman, R. (1985) *J. Magn. Reson.*, **64**, 547–552.

Skerra, A. and Plückthun, A. (1988) *Science*, **240**, 1038–1041.

States, D.J., Haberkorn, R.A. and Ruben, D.J. (1982) *J. Magn. Reson.*, **48**, 286–292.

Takahashi, H., Suzuki, E., Shimada, I. and Arata, Y. (1992) *Biochemistry*, **31**, 2464–2468.

Tomlinson, I.M., Walter, G., Marks, J.D., Llewelyn, M.B. and Winter, G. (1992) *J. Mol. Biol.*, **227**, 776–798.

Uhlen, M., Guss, B., Nilsson, B., Gatenbeck, S., Philipson, L. and Lindberg, M. (1984) *J. Biol. Chem.*, **259**, 1695–1702.

Ward, E.S., Güssow, D., Griffiths, A.D., Jones, P.T. and Winter, G. (1989) *Nature*, **341**, 544–546.

Winter, G. and Milstein, C. (1991) *Nature*, **349**, 293–299.

Wright, P.E., Dyson, H.J., Lerner, R.A., Riechmann, L. and Tsang, P. (1990) *Biochem. Pharmacol.*, **40**, 83–88.

Yokota, T., Milenic, D.E., Whitlow, M. and Schlom, J. (1992) *Cancer Res.*, **52**, 3402–3408.